Science of Sintering, **38** (2006) 239-244

DOI: 10.2298/SOS0603239N

UDK 622.785: 553.689

Analysis of Early-Stage Sintering Mechanisms of Mechanically Activated $BaTiO_3$

M. V. Nikolić[1*)], V. P. Pavlović[2], V. B. Pavlović[3], M. M. Ristić[4]

[1]Center for Multidisciplinary Studies of the University of Belgrade, Kneza Višeslava 1, 11000 Beograd, Serbia

[2]Faculty of Mechanical Engineering, University of Belgrade, Kraljice Marije 16, 11000 Beograd, Serbia

[3]Faculty of Agriculture, University of Belgrade, Beograd, Serbia

[4]Serbian Academy of Sciences and Arts, Knez Mihailova 35, 11000 Beograd, Serbia

Abstract:

Barium-titanate powder was mechanically activated in a planetary-ball mill for 60 and 120 minutes. Non-isothermal sintering of non-activated and activated powder samples was investigated using a dilatometer in the temperature interval from room to 1380°C with three different heating rates (10, 20 and 30°C/min). Early-stage sintering mechanisms for all three types of samples were analyzed, showing significant differences between the non-activated and mechanically activated samples.

Keywords: *$BaTiO_3$, Mechanical activation, Sintering mechanism*

Introduction

Materials based on barium-titanate have excellent dielectric and electromechanical properties and are thus often used in multilayer ceramic capacitors (MLLC), piezoelectric devices, electroluminescent panels, and polymer-matrix composites for integral passive devices. Other applications also include coatings for shielding and electro-static control [1]. In order to reduce particle size and modify physico-chemical properties mechanical activation of initial powders by high-energy ball milling is often used [2]. Soft agglomerates often form in mechanically activated powders as a result of increased surface energy of mechanically activated powders, while the particle morphology remains relatively irregular. The constant heating method has been often used to investigate sintering mechanisms of different materials, such as for example UO_2 [3], Ni-Zn ferrites [4], and CeO_2 [5]. In this paper we have investigated the influence of mechanical activation on non-isothermal sintering of $BaTiO_3$ by analyzing early stage (initial and intermediate stages) sintering mechanisms.

Based on the general equation for isothermal initial-stage sintering proposed by Woolfrey and Bannister [6],

$$\frac{d}{dt}\left(\frac{\Delta L}{L_0}\right) = A_0 \exp\left(-\frac{Q}{RT}\right) \Big/ (\Delta L / L_0)^m \qquad (1)$$

*) Corresponding author: maria@mi.sanu.ac.yu

where $\Delta L/L_0$ is relative shrinkage, t is time A_0 is a constant depending only on the material parameters and sintering mechanisms and m has different values depending on dominant mass transport mechanisms (m=0 for viscous flow m=1 for volume diffusion, m=2 for grain boundary diffusion [7]), Young and Cutler [8] derived several equations for describing initial sintering by measuring powder compact shrinkage at constant heating rates, either using shrinkage or shrinkage-rate. The first using shrinkage is in the following form:

$$(\Delta L / L_0) / T = A_1 \exp\left[-\frac{Q}{(m+1)RT} \right] \tag{2}$$

In logarithmic form:

$$\ln[(\Delta L / L_0) / T] = -\frac{Q}{(m+1)R} \frac{1}{T} + \ln A_1 \tag{3}$$

The second one uses the shrinkage rate in the following form:

$$T^2 d(\Delta L / L_0) / dt = A_2 \frac{Q}{(m+1)R} \frac{1}{T} \cdot \left(\frac{\Delta L}{L_0} \right) \tag{4}$$

where A_1 and A_2 are constants depending only on the material parameters and sintering mechanisms. Both shrinkage and shrinkage-rate equations are used for data analysis [6]. No assumptions are made regarding geometry or the sintering mechanism, except that one rate-controlling mechanism dominates.

The value of m can be obtained using either isothermal or non-isothermal techniques [5]. Woolfrey and Bannister [6] obtained m by performing experiments with different heating rates.

In the case when only one heating rate is used or shrinkage depends on the heating rate the Dorn method is used to determine the instantaneous effect of a small change in temperature on the shrinkage rate [6]. If V_1 is the shrinkage rate at temperature T_1 just before the temperature change and V_2 is the shrinkage rate at T_2 just after the change, then the apparent activation energy of the process responsible for sintering is given by [3,6]:

$$Q = \frac{RT_1T_2}{T_2 - T_1} \ln\left(\frac{T_2V_2}{T_1V_1} \right) \tag{5}$$

This method does not need a theoretical model, as the use of different theoretical equations that depend on the densification state studied is not necessary [3].

Experimental

A commercial $BaTiO_3$ powder (Merck 99.8% purity Ba/Ti ratio of 1:1, mean grain size ~ 1 μm) was used as the starting material. The powder was mechanically activated in a planetary-ball mill in a continuous regime for 60 and 120 minutes. After mechanical activation samples of the powders obtained and the non-activated powder were pressed into pellets 6 mm in diameter with an average thickness of 4 mm. Non-isothermal sintering of these samples was carried out in a dilatometer (Bahr Geratebau GmbH) at three heating rates (10, 20 and 30^{o}C/min) up to 1380^{o}C.

Results and discussion

Fig. 1 shows plots calculated using eq. 4 for the non-activated (fig. 1a) and samples activated for 60 (fig. 1b) and 120 minutes (fig. 1c). According to Woolfrey and Bannister [6] the slope of this plot is correct irrespective of the sintering mechanism.

Differences between the plots calculated for the non-activated and activated samples can be noted. The linear curve parts represent stages in which one sintering mechanism was dominant, while non-linear parts represent transition regions between two mechanisms. According to Young and Cutler [8] a change in the slope could be caused by a particle size distribution, a change in mass transport mechanism or by a change in relation between sintering mechanisms (which is dominant).

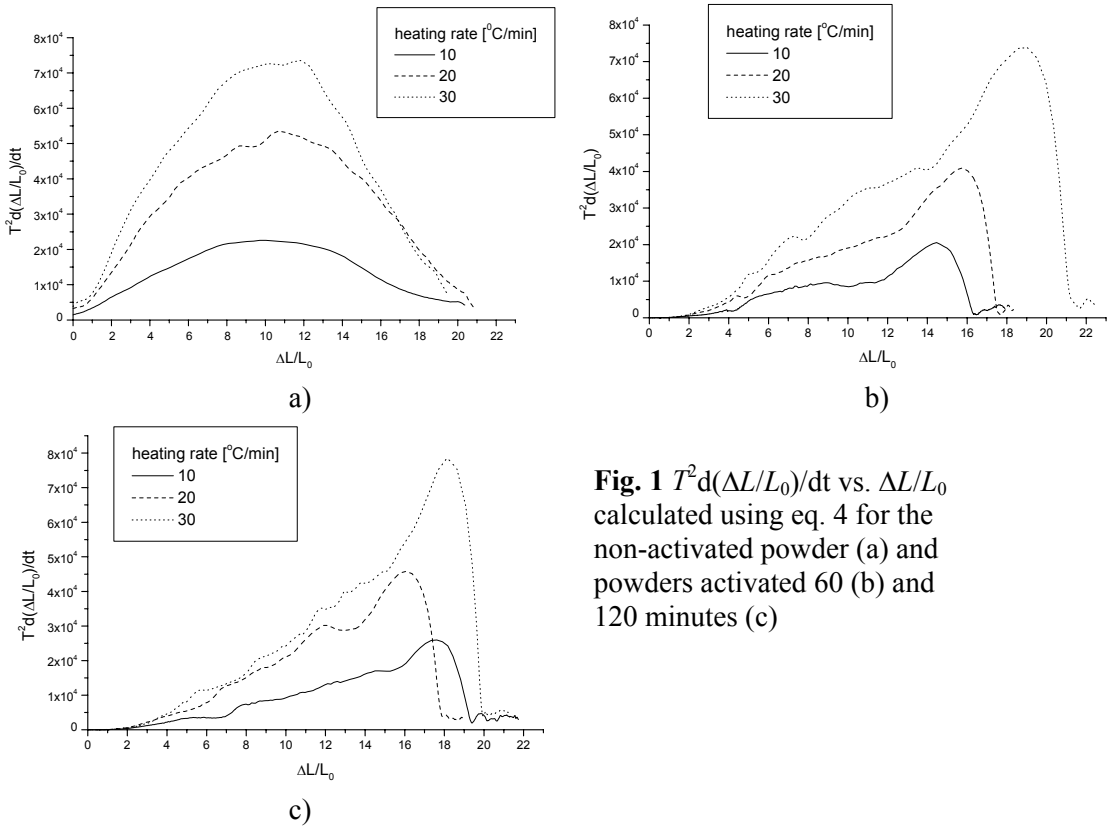

Fig. 1 T^2d($\Delta L/L_0$)/dt vs. $\Delta L/L_0$ calculated using eq. 4 for the non-activated powder (a) and powders activated 60 (b) and 120 minutes (c)

For the non-activated powder shrinkage started at the temperature of 1070°C and there is one linear stage between 2 and 8% in the temperature range of 1150-1210°C. It is followed by a transition region between 1210-1240°C, while the final stage was for shrinkage between 13 and 20%. They were the same irrespective of the heating rate. Both activated powders showed similar behaviour. Shrinkage started at lower temperatures than was the case for the non-activated powder. The early sintering stage until achieving a maximal shrinkage rate is characterized by several segments, while the slope of the final stage of sintering is much steeper for both activated powders compared to the non-activated one.

For the powder activated 60 min three linear curve parts were noted with transition regions in between compared to one for the non-activated powder until the maximum shrinkage rate was achieved. The values of shrinkage and temperature of these stages are given in tab. I. One can note that these three stages occurred at similar temperatures for all three sintering rates though the shrinkage values were different and depended on the heating rate.

Similar behaviour was noted for the powder activated 120 min (three linear stages) and the values obtained are given in tab. I. Compared to the powder activated for 60 minutes the first linear stage started at lower temperatures for the powder activated 120 minutes, while the other two linear stages were at slightly higher temperatures.

Tab. I Shrinkage (denoted as s in %) and temperature of three sintering stages of BaTiO3 powder activated for 60 and 120 minutes where one sintering mechanism is dominant

Powder activated 60 minutes												
stage	heating rate 10 °C/min				heating rate 20 °C/min				heating rate 30 °C/min			
	s_1	s_2	T_1	T_2	s_1	s_2	T_1	T_2	s_1	s_2	T_1	T_2
I	2.73	3.83	945	1027	2.95	4.29	945	1027	2.4	4.37	944	1014
II	4.25	5.21	1050	1084	4.81	5.83	1046	1077	5.52	7.21	1049	1084
III	11.4	14.4	1179	1209	12.3	15.7	1176	1207	14.07	18.8	1168	1207
Powder activated 120 minutes												
stage	heating rate 10 °C/min				heating rate 20 °C/min				heating rate 30 °C/min			
	s_1	s_2	T_1	T_2	s_1	s_2	T_1	T_2	s_1	s_2	T_1	T_2
I	2.05	4.76	854	1046	2.07	5.6	847	1097	2.79	5.35	860	1040
II	6.81	7.63	1113	1133	6.07	6.74	1112	1130	7.69	8.44	1106	1125
III	15.89	17.23	1231	1240	13.65	15.67	1223	1239	15.1	17.69	1215	1236

These differences between shrinkage behaviour for the non-activated and activated powders are in accordance with our previous analysis where we established a correlation between shrinkage and densification rates and microstructure evolution [9]. Then, we divided the increasing part of the densification rate curve for mechanically activated samples into three processes. The first process was attributed to intra-agglomerate particle sintering; the second one to the sintering of grains between the aggregates and the third process was attributed to aggregate sintering. Microstructure analysis also showed differences in the structure of the non-activated powder and the activated ones.

As shrinkage of the activated powders depended on the heating rate Dorn's method (eq. 5) was used to determine apparent activation energy values for both activated powders and the non-activated powder. The values obtained for the non-activated powder and powder activated 60 and 120 minutes are given in tab. II. The apparent activation energy value obtained for the non-activated powder is in accordance with the values determined by Genuist and Haussonne [10]. For the activated powders apparent activation energy values are lower than for the non-activated powder and are similar for both activation times. Mechanical activation led to intensification of transport processes and thus increased sinterability.

Tab. II Values of apparent activation energy and m for non-activated $BaTiO_3$ powder (a) and $BaTiO_3$ powder activated for 60 (b) and 120 (c) minutes, respectively

Powder	I		II		III	
	Q [kJ/mol]	m	Q [kJ/mol]	m	Q [kJ/mol]	m
a	523	0.59				
b	114	2.26	409	3.77	453	2.49
c	110	1.64	380	4.08	516	2.52

Plots of $\ln[\Delta L/L_0]$ versus $1/T$ using eq. 3 in the relative shrinkage range of 2-8% are given in fig. 2. The three curves corresponding to the three different heating rates exhibit almost the same slope. The average of all three slopes is used to calculate the value of the exponent m reflecting the dominant sintering mechanism that is also given in tab. II.

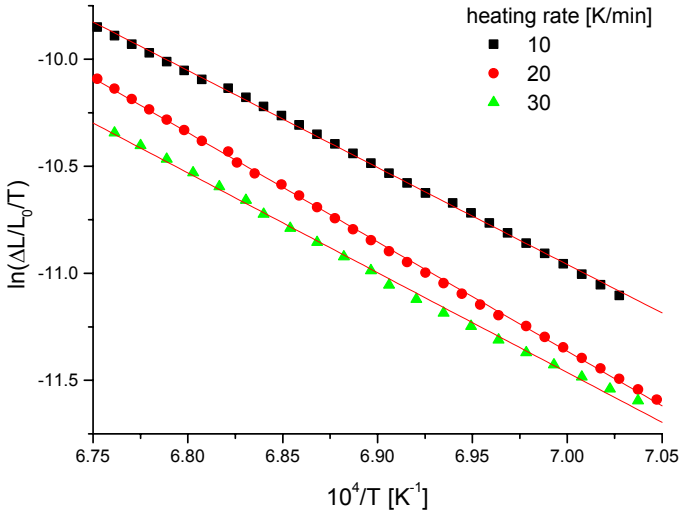

Fig. 2 $\ln(\Delta L/L_0/T)$ versus 1/T for non-activated $BaTiO_3$

The plots of $\ln[\Delta L/L_0]$ versus $1/T$ using eq. 3 in the three analyzed shrinkage ranges for $BaTiO_3$ powder activated 60 and 120 minutes also exhibited almost the same slope for all three heating rates and the average values of m are also given in tab. II. An example is given in fig. 3.

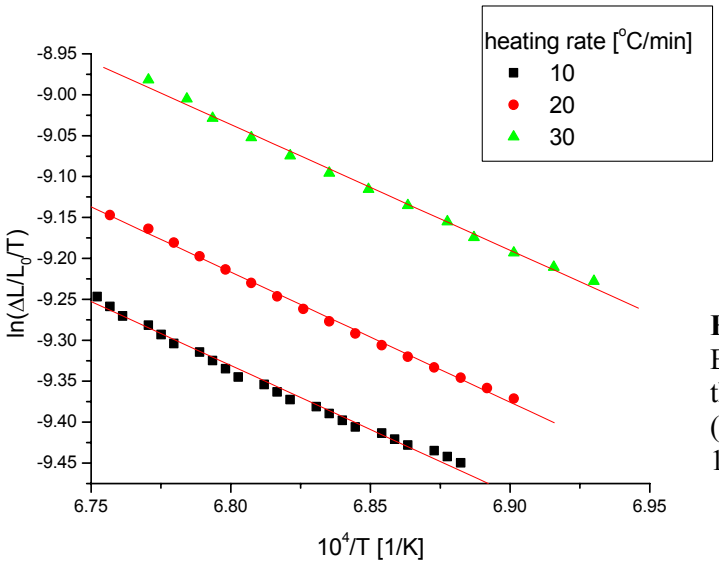

Fig. 3 $\ln(\Delta L/L_0/T)$ versus 1/T for $BaTiO_3$ activated 60 min for the third sintering stage (temperature range of 1179-1209°C)

An analysis of the values obtained for m show that different sintering mechanisms are dominant in the early sintering stage for the case of non-activated and activated powders. According to the definition of m by Woolfrey and Bannister [6] in the case of the non-activated powder it is volume (bulk or lattice) diffusion (m=1), while grain-boundary diffusion is dominant in the case of the activated powders (m≥2).

Conclusion

In this paper early stage (initial and intermediate stages) sintering mechanisms of mechanically activated $BaTiO_3$ powder were analyzed and compared with non-activated

$BaTiO_3$ powder. It was found that the shrinkage rate depended on the heating rate and that the early sintering stage of mechanically activated $BaTiO_3$ consisted of three stages where one sintering mechanism is dominant (grain boundary diffusion) interconnected with transition stages compared to non-activated $BaTiO_3$ where there was only one stage. Apparent activation energies were calculated using Dorn's method and they were lower for the activated powder compared to the non-activated one.

Acknowledgements

The authors would like to express their gratitude to N. Labus for dilatometry measurements.

References

1. S. Venigalla, Am. Ceram. Soc. Bull. 6 (2001) 63.
2. D. L. Zhang, Materials Science 49 (2004) 537.
3. Ph. Dehaudt, L. Bourgeois, H. Chevrel, J. Nucl. Mater. 299 (2001) 250.
4. A. C. F. de Melo Costa, E. Tortella, E. Fagury Neto, M. R. Morelli, R. H. G.A. Kiminami, Materials Research 7 (2004) 523.
5. Z. Tianshu, P. Hing, H. Huang, J. Kilner, J. Mater. Sci., 37 (2002) 997.
6. J. Woolfrey, M. J. Bannister, J. Am. Ceram. Soc., 55 (1972) 390.
7. J. L. Woolfrey J. Am. Ceram. Soc., 55 (1972) 383.
8. W. S. Young, I. B. Cutler, J. Am. Ceram. Soc, 53 (1970), 659.
9. V. P. Pavlović, M. V. Nikolić, V. B. Pavlović, N. Labus, Lj. Živković, B. D. Stojanović, Ferroelectrics, 319 (2005), 75.
10. C. Genuist, F. J. M. Haussonne, Ceramics International, 14 (1988), 169.

Садржај: *Прах баријум-титаната је механички активиран у планетарном млину са куглицама 60 и 120 минута. Неизотермско синтеровање неактивираног и активираних узорака проучено је у дилатометру у температурском интервалу од собне до 1380°C са три различите брзине загревања (10, 20 и 30°C/мин). Механизми раних стадијума синтеровања су анализирани за сва три типа узорака и уочене су значајне разлике између неактивираних и механички активираних узорака.*
Кључне речи: *BaTiO3, механичка активација, механизам синтеровања.*